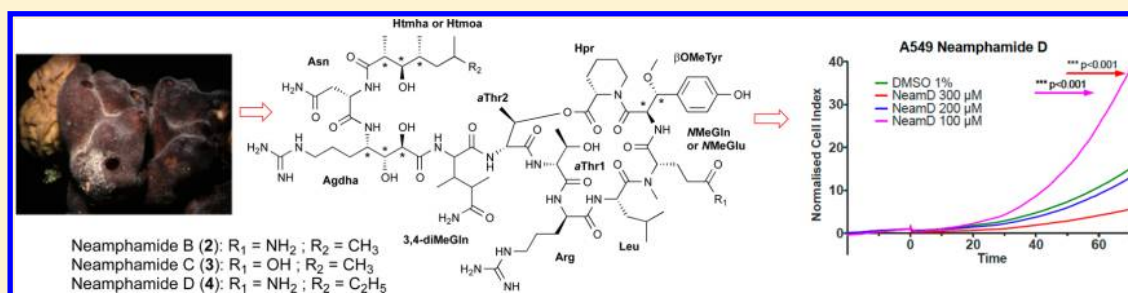


# Cytotoxic Cyclic Depsipeptides from the Australian Marine Sponge *Neamphius huxleyi*

Trong D. Tran, Ngoc B. Pham, Gregory Fechner, Dusan Zencak, Hoan T. Vu, John N. A. Hooper, and Ronald J. Quinn\*

Eskitis Institute, Griffith University, Brisbane, Queensland 4111, Australia

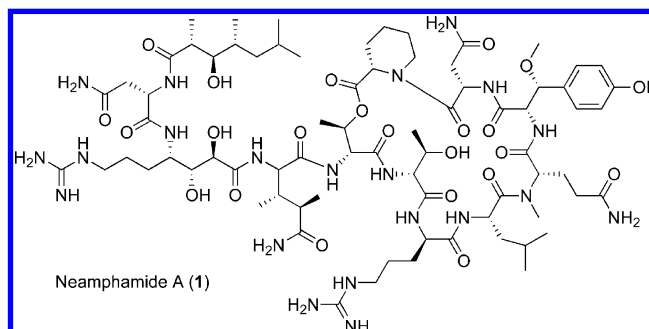
**S** Supporting Information



**ABSTRACT:** Three new cyclic depsipeptides, neamphamides B (2), C (3), and D (4), were isolated from the Australian sponge *Neamphius huxleyi*. The planar structural characterization of these molecules was elucidated using 2D NMR experiments and ESI-FTICR-MS<sup>n</sup>. Their configurations were determined by Marfey's method and J-based NMR analysis. These new metabolites inhibited the growth of human cell lines (A549, HeLa, LNCaP, PC3, and NFF) with IC<sub>50</sub> values ranging from 88 to 370 nM. However, neamphamide D causes A549 cell proliferation at subcytotoxic doses and should be treated cautiously as a cytotoxic compound.

Marine organisms have proven to be a pool of diverse chemical structures with a range of biological activities. Callipeltin A isolated from the sponge *Callipelta* sp. in 1996 was the first peptide from marine sponges possessing the previously unknown residues (2*S*,3*S*,4*R*)-3,4-dimethylglutamine (3,4-diMeGln), (2*S*,3*R*)-β-methoxytyrosine (βOMeTyr), (2*R*,3*R*,4*S*)-4-amino-7-guanidino-2,3-dihydroxyheptanoic acid (Agdha), and (2*R*,3*R*,4*R*)-3-hydroxy-2,4,6-trimethylheptanoic acid (Htmha).<sup>1</sup> Sharing these atypical units, 31 peptides and depsipeptides have been identified in marine sponges so far, including callipeltins A–M from *Callipelta* sp. and *Latrunclia* sp.,<sup>2–5</sup> homophymines A–E and A1–E1 from *Homophymia* sp.,<sup>6,7</sup> mirabamides A–D from *Siliquariaspongia mirabilis*,<sup>8</sup> papuamides A–D and theopapuamide from *Theonella mirabilis* and *T. swinhoei*,<sup>9,10</sup> and neamphamide A from *Neamphius huxleyi*.<sup>11</sup> These peptides have been reported to exhibit strong antifungal,<sup>8</sup> anti-HIV,<sup>1,6,9,11</sup> and cytotoxic<sup>7,10</sup> activities.

The genus *Neamphius*, one of six sponge genera in the family Alecionidae (*Alectona*, *Delectona*, *Dotona*, *Neamphius*, *Scolopes*, and *Spiroxya*), was first described by Sollas in 1888.<sup>12</sup> Until now, only two compounds have been identified from the sponge *Neamphius huxleyi*. Neamphine, a sulfur-containing aromatic heterocycle, was reported to have cytotoxic activity in 1991.<sup>13</sup> The second metabolite, neamphamide A (1), isolated from the Papua New Guinea sponge *N. huxleyi*, has been reported to possess an anti-HIV activity with an IC<sub>50</sub> of 28 nM.<sup>11</sup>



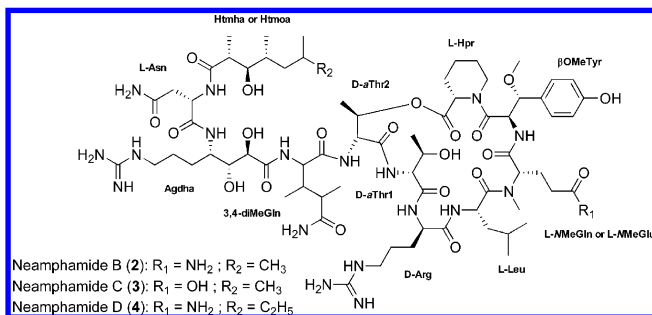
In the search for potential antitumor compounds from marine organisms, a single fraction derived from a prefractionated extract of the Australian sponge *N. huxleyi* was identified as having potent activities against lung (A549), cervical (HeLa), and prostate (LNCaP and PC3) cancer cell lines. This paper reports the isolation and structure elucidation of three new cyclic depsipeptides, neamphamides B (2), C (3), and D (4), along with their cytotoxic activity.

## RESULTS AND DISCUSSION

LC/MS analysis of the single active fraction of *N. huxleyi* extract indicated this fraction contained ion peaks at (+) *m/z* 788.0, 788.5, and 795.0 in the (+)-LRESIMS spectrum. Large-

**Received:** September 20, 2012

scale isolation was then performed on the freeze-dried and ground sample of *N. huxleyi* (5 g). A combined CH<sub>2</sub>Cl<sub>2</sub>/MeOH extract was chromatographed on C18 bonded silica HPLC (MeOH/H<sub>2</sub>O/0.1% TFA). Mass-guided identification afforded three new compounds, neamphamides B–D (2–4).



Neamphamide B (2) was purified as a colorless, amorphous powder. The (+)-HRESIMS displayed a divalent molecular ion [M + 2H]<sup>2+</sup> at *m/z* 787.9463 and a molecular ion [M + H]<sup>+</sup> at *m/z* 1574.8935, which was consistent with the molecular formula C<sub>71</sub>H<sub>119</sub>N<sub>19</sub>O<sub>21</sub>. Compound 2 showed poor solubility in acetone, pyridine, and acetonitrile. The <sup>1</sup>H and <sup>13</sup>C NMR spectra in DMSO-*d*<sub>6</sub> or combined solvent systems with DMSO-*d*<sub>6</sub> (CH<sub>3</sub>CN-*d*<sub>3</sub>/DMSO-*d*<sub>6</sub>; Me<sub>2</sub>CO-*d*<sub>6</sub>/DMSO-*d*<sub>6</sub>; C<sub>3</sub>H<sub>5</sub>N-*d*<sub>5</sub>/DMSO-*d*<sub>6</sub>) exhibited broadened peaks with two or three sets of signals. By employing MeOH-*d*<sub>4</sub>, the <sup>1</sup>H and <sup>13</sup>C NMR spectra were recorded as a single set of well-resolved resonances. Therefore, MeOH-*d*<sub>4</sub> was used for a series of 1D- and 2D-NMR experiments (<sup>1</sup>H NMR, <sup>13</sup>C NMR, COSY, ROESY, TOCSY, HSQC, HMBC, HSQC-TOCSY, and HSQMBC) for structure elucidation for compound 2. However, exchangeable protons could not be observed in MeOH-*d*<sub>4</sub>. MeOH-*d*<sub>3</sub> was then utilized as an alternative NMR solvent for <sup>1</sup>H NMR, <sup>13</sup>C NMR, COSY, ROESY, HSQC, and HMBC spectra to confirm the structure. Good resolutions with sharp exchangeable signals were obtained in MeOH-*d*<sub>3</sub> only after converting this compound from its formic acid salt to the neutral form with ammonium hydroxide.

Combined data from the <sup>13</sup>C NMR and HSQC spectra indicated that this compound contained 14 carbonyls between δ<sub>C</sub> 171.2 and 181.0 ppm; four quaternary carbons at δ<sub>C</sub> 158.8, 158.8, 158.7, and 129.7 ppm; four aromatic carbons (δ<sub>C</sub> 131.1, 131.1, 116.3, and 116.3 ppm); six methine carbons bearing an oxygen atom (δ<sub>C</sub> 84.3, 79.4, 75.6, 73.0, 72.5, and 67.1 ppm); 10 α-methine carbons (δ<sub>C</sub> 51.2–64.0 ppm); one methoxy group at δ<sub>C</sub> 57.1 ppm (δ<sub>H</sub> 3.14 ppm); one *N*-methyl signal at δ<sub>C</sub> 30.8 ppm (δ<sub>H</sub> 2.99 ppm); 10 methyl carbons (δ<sub>C</sub> 24.9, 23.7, 22.9, 21.5, 20.3, 17.4, 15.7, 15.6, 14.9, and 14.8 ppm); and another 21 aliphatic carbons. The peptidic nature of 2 was established by the existence of amide NH protons at δ<sub>H</sub> 6.60–9.15 ppm, observed in the MeOH-*d*<sub>3</sub> <sup>1</sup>H NMR spectrum.

Interpretation of the 2D-NMR data led to the assignment of 10 amino acid units, one arginine (Arg), one asparagine (Asn), one *N*-methylglutamine (NMeGln), one homoproline (Hpr), one leucine (Leu), two threonines (Thr), one β-methoxytyrosine (5, β-OMeTyr), one 3,4-dimethylglutamine (3,4-diMeGln), one 4-amino-7-guanidino-2,3-dihydroxyheptanoic acid (6, Agdha), and one 3-hydroxy-2,4,6-trimethylheptanoic acid (7, Htmha). The two basic guanidine functionalities in Agdha and Arg moieties explained the formation of the doubly charged molecular ion. Analysis of HMBC and ROESY correlations of the methine protons showed that the nine

amino acids and the acid Htmha residue assembled in a sequence β-OMeTyr-NMeGln-Leu-Arg-Thr1-Thr2-3,4-diMeGln-Agdha-Asn-Htmha (Figure 1). The ROESY cross-

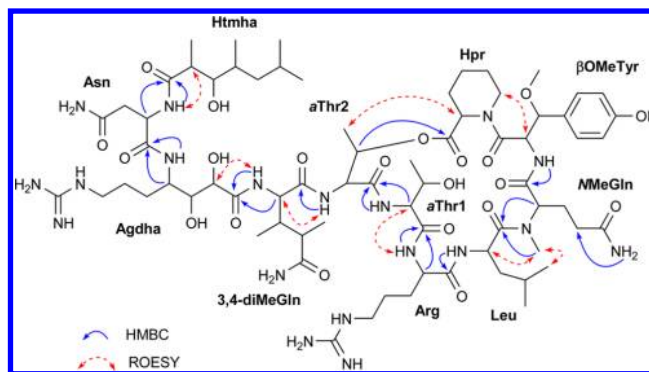


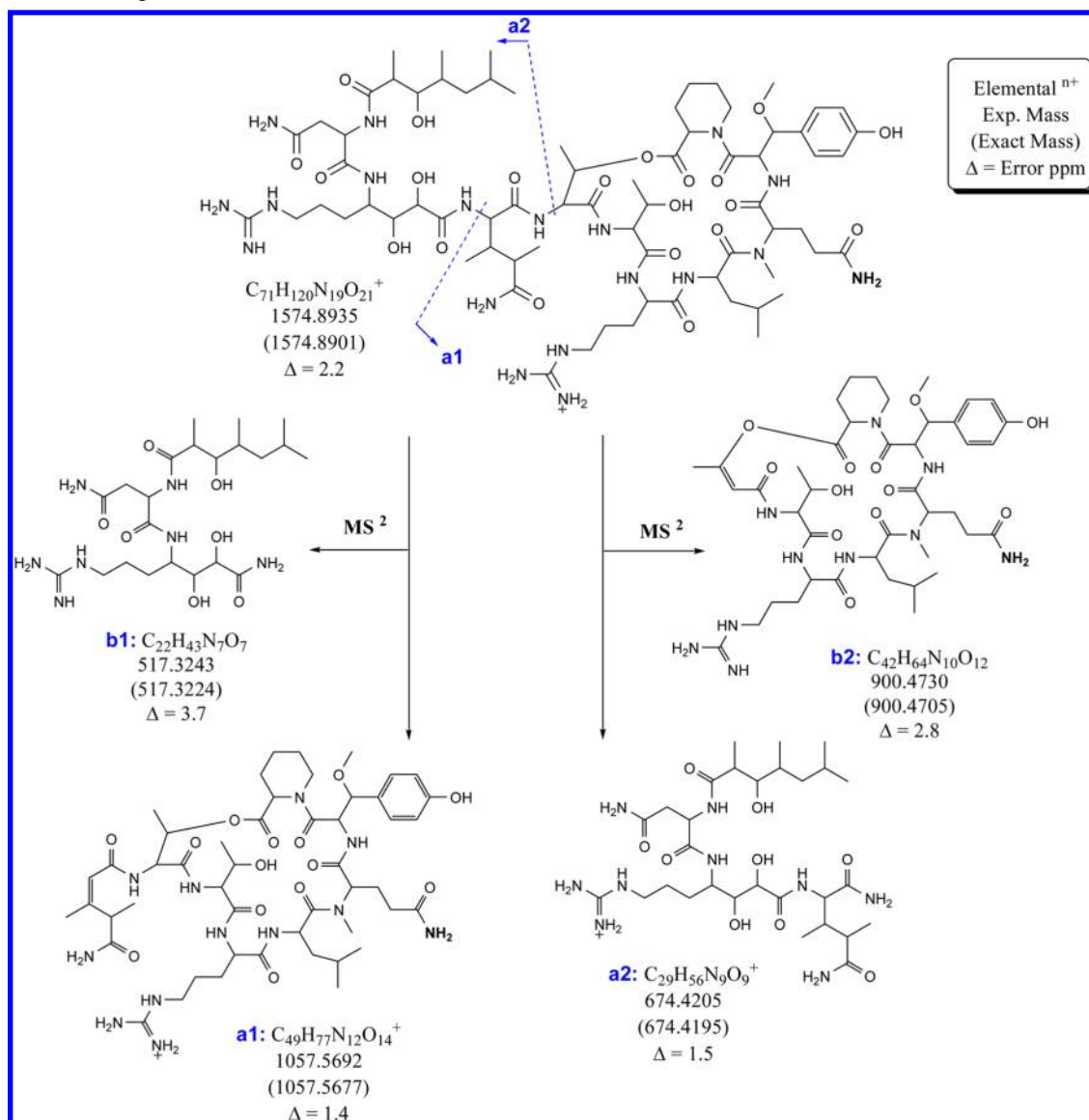
Figure 1. Key HMBC and ROESY correlations of 2.

peak between Hpr-H6 (δ<sub>H</sub> 3.85 ppm) and β-OMeTyr-H2 (δ<sub>H</sub> 5.02 ppm) established the connectivity of the remaining Hpr unit to the β-OMeTyr moiety through an amide linkage. The macrocyclic ring system of 2 was completed by the connectivity between Thr2 and Hpr units, established by the observed HMBC correlation from Thr2-H3 (δ<sub>H</sub> 5.61 ppm) to Hpr-C1 (δ<sub>C</sub> 171.3 ppm).

The complete structure of 2 was confirmed by utilizing electrospray ionization Fourier transform ion cyclotron resonance mass spectrometry (ESI-FTICR-MS<sup>n</sup>). Direct FTMS<sup>2</sup> analysis of the singly charged parent ion of 2 (*m/z* 1574.8935) produced two singlet fragments at *m/z* 1057.5692 and 674.4205 (Scheme 1). The mass difference (517.3243 Da) between the MS<sup>1</sup> pseudomolecular ion and the MS<sup>2</sup> fragment ion **a1** (*m/z* 1057.5692) corresponds to the loss of a neutral molecule **b1** (C<sub>22</sub>H<sub>43</sub>N<sub>7</sub>O<sub>7</sub>). Likewise, the loss of the unique elemental formula C<sub>42</sub>H<sub>64</sub>N<sub>10</sub>O<sub>12</sub> (**b2**) was also deduced from the observation of the highly abundant fragment ion at 674.4205 (**a2**). The fragments obtained by ESI-FTICR-MS<sup>2</sup> experiment further confirmed the structure of 2.

The absolute configurations of seven amino acid constituents in 2, D-Arg, L-Asn, L-NMeGln, L-Hpr, L-Leu, and two D-*allo*-Thr (D-*a*Thr), were assigned by Marfey's analysis.<sup>11,14</sup> The ion peak of the β-OMeTyr amino acid (5) was not observed in either the acid hydrolysate solution or its Marfey derivatives. This problem was previously seen with the hydrolysis of those peptides containing the β-OMeTyr unit under strong acidic conditions.<sup>1,8,9</sup> Thus, *J*-based NMR configurational analysis (Murata's method)<sup>15–17</sup> was applied in the assignment of its relative configurations (Figure 2). The <sup>3</sup>J<sub>H–H</sub> coupling constants were obtained from the <sup>1</sup>H NMR spectrum, while accurate measurements of <sup>2,3</sup>J<sub>H–C</sub> were extracted from 2D-NMR spectra (HSQC-TOCSY and HSQMBC). A ROESY experiment in MeOH-*d*<sub>3</sub> was also carried out in order to assist the establishment of the final configurations. The large coupling value of 9.6 Hz between β-OMeTyr-H2 and β-OMeTyr-H3 pointed to their *anti* orientation relationship. A ROESY correlation from β-OMeTyr-NH at δ<sub>H</sub> 8.23 ppm to β-OMeTyr-H5 at δ<sub>H</sub> 7.22 ppm and no ROESY signal between β-OMeTyr-NH and β-OMeTyr-OMe supported the interpretation of the *erythro* relative configuration for this β-OMeTyr residue.

Here the configurational assignment for the β-OMeTyr unit in 2 was different from that in neamphamide A (1), although

Scheme 1. FTMS<sup>2</sup> Fragmentations and Related Neutral Losses of 2

they were from the same species. The  $\beta$ -OMeTyr-H3 in neamphamide A determined as (*R*)- $\beta$ -OMe-L-Tyr showed a broad singlet signal at  $\delta_{H3}$  5.03 ppm, while the equivalent proton assigned for (*R*)- $\beta$ -OMe-D-Tyr in papuamide B (Figure S1 in Supporting Information) showed a doublet at  $\delta_{H3}$  4.24 ppm with the vicinal coupling constant of 9.3 Hz. In comparison with published NMR data of the known absolute configurational  $\beta$ -OMeTyr residue in other peptides (Table 1), it was seen that the coupling patterns and resonances of the  $\beta$ -OMeTyr in 2 ( $\delta_{H3}$  4.47 ppm,  $J = 9.6$  Hz) were similar to those reported for (*R*)- $\beta$ -OMe-D-Tyr. So far, only two out of four possible stereoisomers of the  $\beta$ -OMeTyr amino acid, (*R*)- $\beta$ -OMe-D-Tyr and (*R*)- $\beta$ -OMe-L-Tyr, have been discovered in natural products.<sup>20</sup> From this evidence, the relative configuration of the  $\beta$ -OMeTyr residue in 2 is proposed as (*R*<sup>\*</sup>)- $\beta$ -OMe-D-Tyr (i.e., (*2R*<sup>\*</sup>,*3R*<sup>\*</sup>)-3-methoxytyrosine).

*J*-based NMR configurational analysis was also used to determine the relative configuration of Agdha (6) and Htmha (7) (Figure 2). A large  $^3J_{H2-H3}$  of 9.6 Hz in the Agdha unit indicated an *anti* orientation between these protons. No ROE effect was detected from 2-OH to 3-OH, while the ROESY

spectrum showed a correlation between Agdha-2OH and Agdha-H4. This supported a C2–C3 *erythro* configuration. A *gauche* relationship between Agdha-H3 and Agdha-H4 was deduced due to their small coupling constant  $^3J_{H3-H4}$  of 0.6 Hz. The small vicinal coupling constants  $^3J_{H3-C5}$  and  $^3J_{H4-C2}$  confirmed the assignment of a *threo* configuration at C3–C4 in the Agdha moiety. Hence, the configurations of the Agdha residue (6) in 2 were established as (*2R*<sup>\*</sup>,*3R*<sup>\*</sup>,*4S*<sup>\*</sup>)-Agdha.

The large magnitude of  $^3J_{H2-H3} = 9.6$  Hz in the Htmha residue (7) accounted for an *anti* rotamer at two stereocenters, C<sub>2</sub> and C<sub>3</sub> (Figure 2). No ROE effect from 3-OH to Htmha-H8 indicated a C2–C3 *erythro* configuration. The observation of a ROE correlation between Htmha-H8 and Htmha-H4 added further strength to this interpretation. A *gauche* rotamer between Htmha-H3 and Htmha-H4 was deduced due to an obtained small vicinal coupling of  $^3J_{H2-H3} = 3.6$  Hz. Other values of heteronuclear coupling constants (Figure 2) were in agreement with a *gauche*<sup>+</sup> rotamer in the *erythro* relative configuration. The configurations of 7 were, therefore, assigned as (*2R*<sup>\*</sup>,*3R*<sup>\*</sup>,*4R*<sup>\*</sup>)-Htmha.

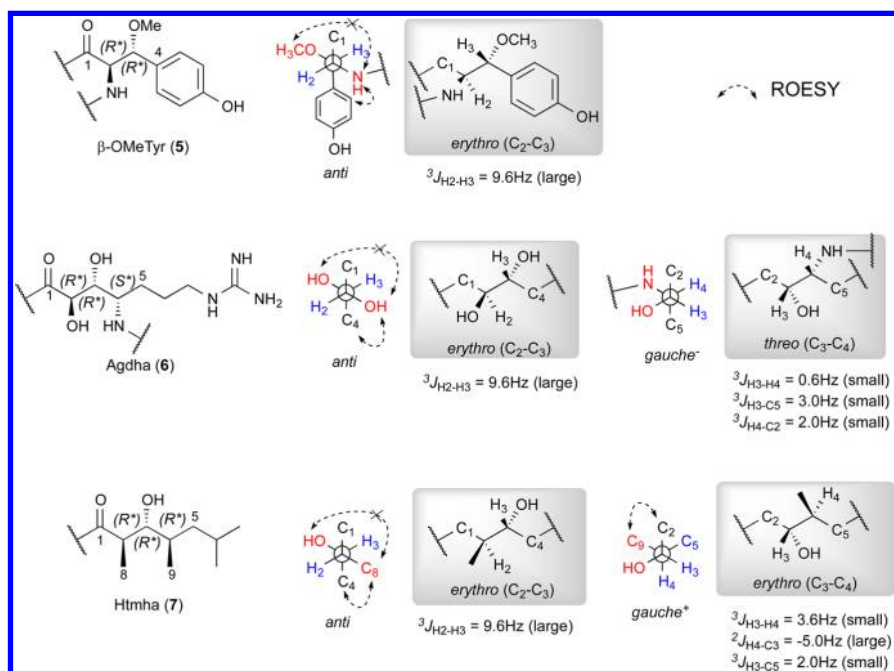
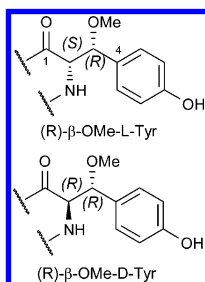


Figure 2. Relative configurations for the  $\beta$ -OMeTyr (5), Agdha (6), and Htmha (7) residues.

Table 1. NMR Comparison of the  $\beta$ -OMeTyr Residue



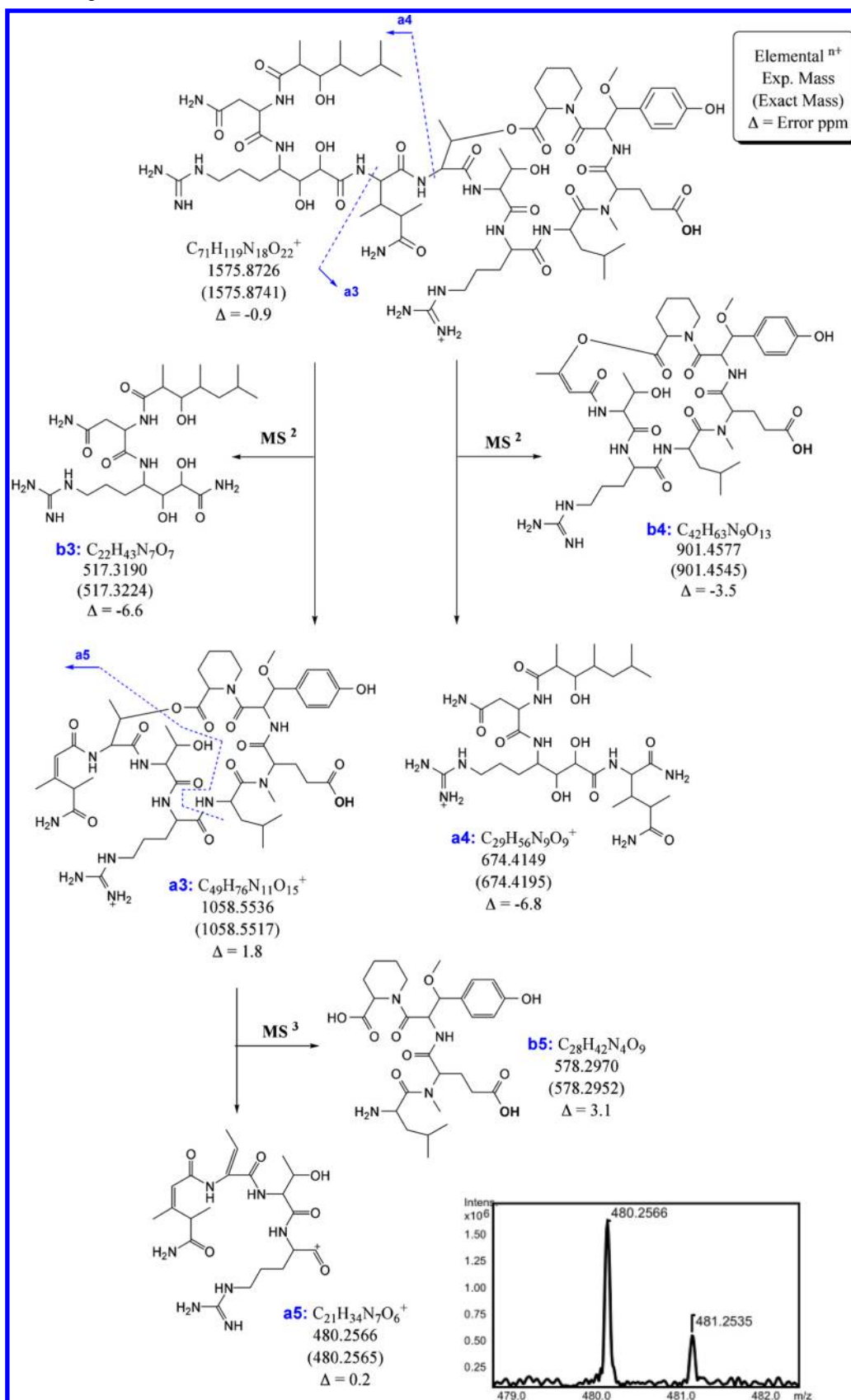
natural product	$^3J_{H2-H3}$ (Hz)	$\delta_{H2}$ (ppm)	$\delta_{C2}$ (ppm)	$\delta_{H3}$ (ppm)	$\delta_{C3}$ (ppm)	configuration
neamphamide A <sup>11</sup>	— <sup>a</sup>	4.67	60.3	5.03	81.9	(2S,3R) <sup>18</sup>
callipeltin A <sup>1</sup>	9.5 <sup>b</sup>	5.01	53.5	4.55	84.0	(2R,3R) <sup>19</sup>
papuamide B <sup>9</sup>	9.3 <sup>b</sup>	5.18	53.4	4.24	84.7	(2R,3R) <sup>18</sup>
mirabamide A <sup>8</sup>	9.7 <sup>c</sup>	5.31	52.1	4.29	84.6	(2R,3R) <sup>8</sup>
neamphamide B (2)	9.6 <sup>b</sup>	5.02	52.9	4.47	84.0	(2R,3R) or (2S,3S)

<sup>a</sup>Broad singlet. <sup>b</sup>Recorded in MeOH-*d*<sub>4</sub> or MeOH-*d*<sub>3</sub>. <sup>c</sup>Recorded in CD<sub>3</sub>CN/H<sub>2</sub>O (5:1).

Neamphamide C (3) was isolated as a colorless, amorphous solid. The (+)-HRESIMS showed a divalent molecular ion  $[M + 2H]^{2+}$  at  $m/z$  788.4396 and a molecular ion peak at  $m/z$  1575.8726 ( $[M + H]^+$ ) corresponding to the molecular formula C<sub>71</sub>H<sub>118</sub>N<sub>18</sub>O<sub>22</sub>. This indicated that 3 differs from 2 in the presence of an OH group in the place of an NH<sub>2</sub> group. Consequently, one of the carboxamide groups in three amino acid residues (NMeGln, 3,4-DiMeGln, and Asn) should be replaced by a carboxyl group in 3. The 1D- and 2D-NMR data measured in MeOH-*d*<sub>4</sub> of both compounds were similar. Attempts to interpret the NMR spectroscopic data in MeOH-*d*<sub>3</sub> were unsuccessful since the data did not provide well-resolved exchangeable signals. Marfey's analysis of 3 showed the presence of D-Arg, L-Asn, L-Hpr, L-Leu, two D-*a*Thr, and one L-N-methylglutamic acid (L-NMeGlu) residue, while the peak corresponding to L-NMeGln was not seen. This indicated 3 differs from 2 at the L-NMeGlu residue. Detailed NMR analysis of 3 revealed the key HMBC correlations from NMeGlu-NCH<sub>3</sub>

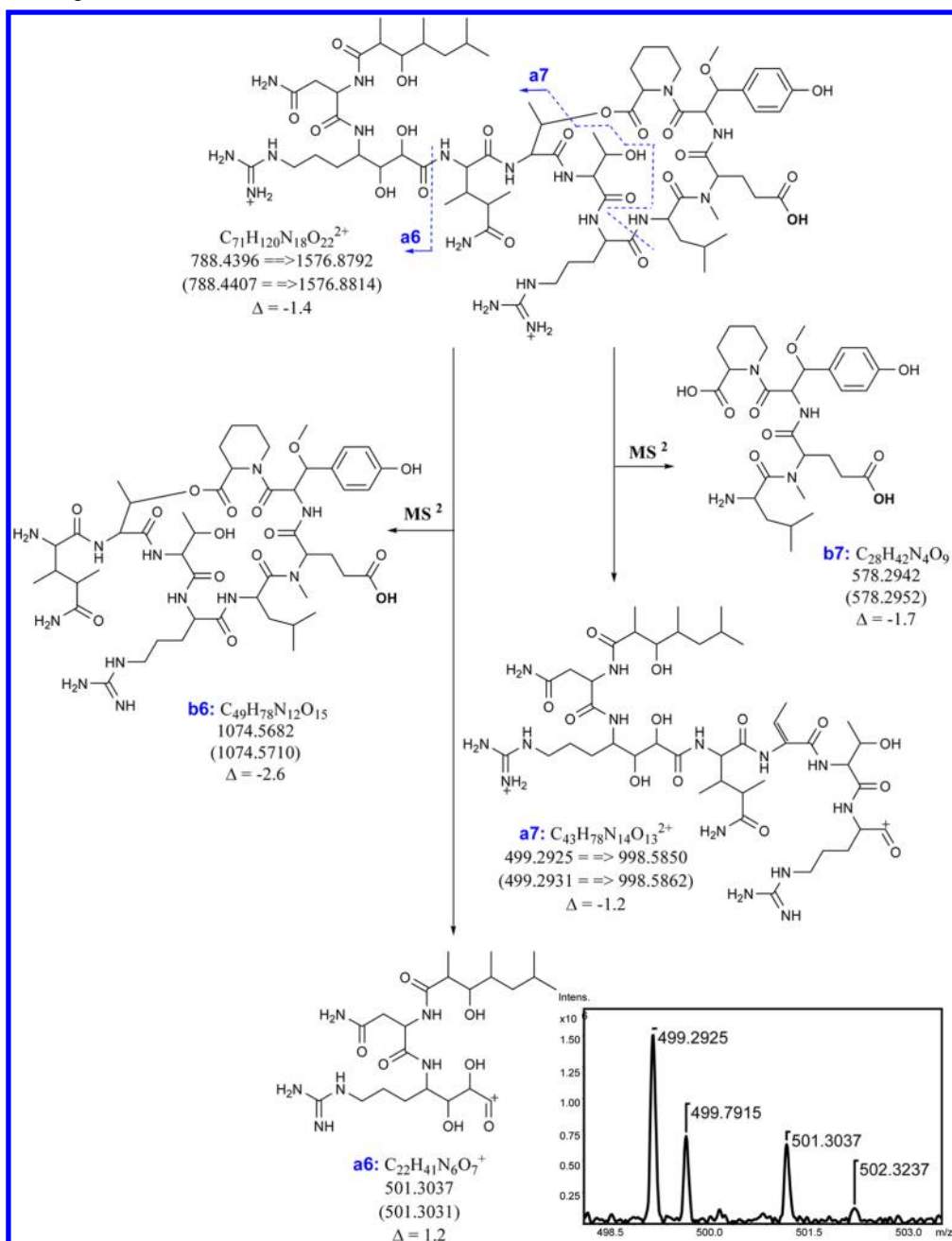
to Leu-C1, Arg-H2 to *a*Thr1-C1, *a*Thr1-H2 to *a*Thr2-C1, 3,4-diMeGln-H2 to Agdha-C1, *a*Thr2-H3 to Hpr-C1, and Asn-H2 to Htmha-C1 and a key ROESY correlation between Hpr-H6 and  $\beta$ OMeTyr-H2, suggesting amino acids in 3 were aligned in the same sequence as those in 2. Structural elucidation of 3 was confirmed by multiple-stage ESI-FTICR-MS<sup>n</sup>.

The sequential fragmentations observed for 3 are described in Scheme 2. The singly charged parent ion of 3 ( $m/z$  1575.8726) was fragmented into two significant ions at  $m/z$  1058.5536 (a3) and 674.4149 (a4). Compared with the fragment a1 in 2, fragment a3 was 1 amu higher, while the elemental formula assigned for a4 was the same as a2 in 2. This indicated that the OH group replaced the NH<sub>2</sub> group in the residue NMeGln (Scheme 2). A FTMS<sup>3</sup> study for the  $m/z$  1058.5536 ion showed a significant singly charged ion at  $m/z$  480.2566 demonstrating the loss of the b5 moiety, which contained the residue NMeGlu (Scheme 2).

Scheme 2. FTMS<sup>2,3</sup> Fragmentations and Related Neutral Losses of 3 (isolated  $m/z$  1575.8726)

Similar evidence for the presence of the NMeGlu residue was also obtained when a doubly charged parent ion ( $m/z$  788.4396) was isolated for the MS<sup>2</sup> stage of fragmentation

(Scheme 3). Two other important fragments, one singly charged ion a6 ( $m/z$  501.3037) and one doubly charged ion a7 ( $m/z$  499.2925), were observed in the FTMS<sup>2</sup> spectrum.

Scheme 3. FTMS<sup>2</sup> Fragmentations and Related Neutral Losses of **3** (isolated  $m/z$  788.4396)

Detailed analysis of MS data indicated that these fragments were formed as a result of the elimination of two neutral moieties **b6** and **b7** from the parent molecule. All information from ESI-FTICR-MS<sup>n</sup> definitely confirmed the presence of the NMeGlu residue in **3**.

Other stereocenters of the  $\beta$ -OMeTyr, Agdha, and Htmha moieties in **3** were assumed to be identical to the corresponding asymmetric centers in **2** on the basis of similar chemical shifts and ROE patterns. Thus, the complete structure of **3** was established.

Neamphamide D (**4**) was obtained as a colorless, amorphous powder. The (+)-HRESIMS displayed a signal at  $m/z$  1588.9052 corresponding to the molecular formula  $C_{72}H_{121}N_{19}O_{21}$ , 14 mass units more than that of **2**, corresponding to one methylene group excess. NMR analysis indicated the residues in **4** were similar to those in **2** with the

presence of Arg, Asn, NMeGln, Hpr, Leu, Thr,  $\beta$ -OMeTyr, 3,4-DiMeGln, and Agdha. The only difference between **4** and **2** was the replacement of the 3-hydroxy-2,4,6-trimethylheptanoic acid unit (**7**, Htmha) in **2** by a 3-hydroxy-2,4,6-trimethyloctanoic acid residue (**8**, Htmoa, Figure 3) in **4**. The spin system of the Htmoa moiety was deduced from COSY and TOCSY analysis.

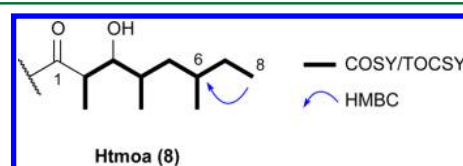
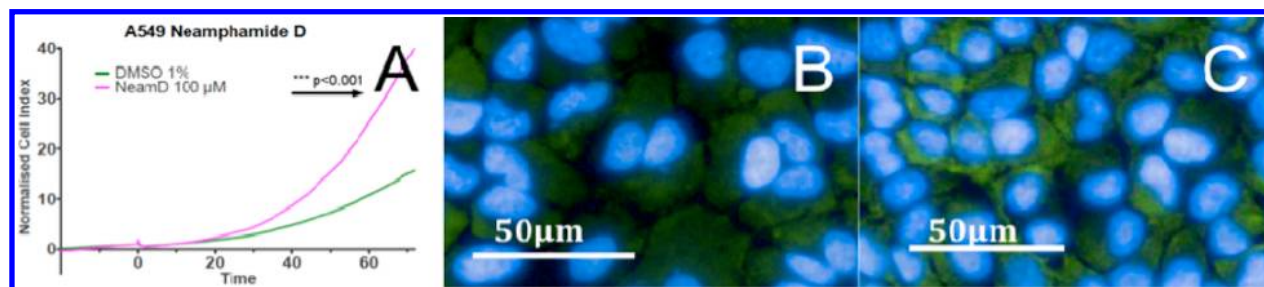


Figure 3. Htmoa unit of **4** with key COSY/TOCSY and HMBC correlations.

Table 2. Cytotoxicity Evaluation for Compounds 2–4<sup>a</sup>

compound	A549	HeLa	LNCaP	PC3	HEK	NFF
2	130 ± 11	110 ± 8.1	230 ± 9.6	170 ± 13	200 ± 26	370 ± 18
3	131 ± 3.5	170 ± 19	190 ± 10	110 ± 4.1	160 ± 31	260 ± 16
4	91 ± 18	210 ± 6.3	110 ± 7.5	130 ± 20	88 ± 13	150 ± 9.2
vincristine sulfate	20 ± 1.9	36 ± 3.5	6.1 ± 0.72	15 ± 1.1	31 ± 3.7	17 ± 3.2

<sup>a</sup>Each IC<sub>50</sub> was determined as the mean ± SD of two independent experiments with triplicate determinations for each concentration.



**Figure 4.** (A) Increased cell index of compound 4 (100 nM) on A549. (B) Control cell proliferation. (C) Increased A549 cell proliferation under the influence of compound 4 (100 nM, 48 h).

The observed key HMBC correlation from Htmoa-H8 ( $\delta_{\text{H}}$  0.90 ppm) to Htmoa-C6 ( $\delta_{\text{C}}$  32.6 ppm) as well as a triplet pattern of Htmoa-H8 ( $J = 7.2$  Hz) confirmed this assignment.

Compound 4 had the same absolute configurations of the seven amino acids as those in 2, D-Arg, L-Asn, L-NMeGln, L-Hpr, L-Leu, and two D-*allo*-Thr (D-*a*Thr), using Marfey's method. Due to insufficient sample quantity, the HSQMBC and HSQC-TOCSY spectra of 4 at Agdha and Htmoa residues were not well-resolved enough for  $J$ -based configurational analysis. On the basis of biogenetic considerations the configuration of Agdha was proposed to be (2*R*\*,3*R*\*,4*S*\*)-Agdha as in 2.

The cytotoxicity of neamphamides B–D (2–4) was evaluated on a panel of human cancer and noncancer cell lines (Table 2). The results demonstrated that these cyclic depsipeptides possessed potent cytotoxic activities, with IC<sub>50</sub> values ranging from 88 to 370 nM.

To get a deeper knowledge about the activities of the compounds, a real-time assessment of cell function or viability using impedance readout was undertaken. The extent of impedance change (cell index) reflects the number of cells inside the well and/or the morphological and adhesive features of the cells, and the shape of the curve can, in some cases, predict the mechanism of action of the compounds tested.<sup>21,22</sup> All three compounds were tested on A549, PC3, and NFF cells at 100, 200, and 300 nM, a range of concentrations close to the IC<sub>50</sub>'s that were determined using the Alamar blue assay. The real-time cell analysis confirmed the compounds were non-selective and failed to identify any mechanism. Interestingly, cell index increased at some of the lower doses for A549 cells (Figure 4). The reason for the increased cell index using impedance readout can be due to increased cell numbers or increased cell size. Confocal imaging was then used to identify the causes. The image showed the effect was due to increased cell numbers. Taken together with the real-time cell analysis there was a prolonged increase in cell numbers for 72 h. This class of compounds should be treated cautiously as cytotoxic compounds, as they may cause cell proliferation at subcytotoxic doses.

In summary, three new depsipeptides, neamphamides B–D, were discovered from the sponge *N. huxleyi*. Notably, structural

analysis indicated a different configuration in the  $\beta$ -OMeTyr residue between neamphamides B–D ((*R*)- $\beta$ -OMe-D-Tyr) and neamphamide A ((*R*)- $\beta$ -OMe-L-Tyr). These three new compounds showed strong cytotoxicity against a panel of human cell lines. Neamphamide D caused A549 cell proliferation at subcytotoxic doses.

## EXPERIMENTAL SECTION

**General Experimental Procedures.** Optical rotations were measured on a JASCO P-1020 polarimeter (10 cm cell). UV and IR spectra were recorded on a CAMSPEC M501 UV/vis spectrophotometer and Bruker Tensor 27 FT-IR spectrometer, respectively. NMR spectra were recorded at 30 °C on a Varian Inova 600 MHz spectrometer. The <sup>1</sup>H and <sup>13</sup>C chemical shifts were referenced to the CD<sub>3</sub>OD and CD<sub>3</sub>OH solvent peaks at  $\delta_{\text{H}}$  3.31 and  $\delta_{\text{C}}$  49.15 ppm. Standard parameters were used for the 2D NMR spectra obtained, which included gCOSY, gHSQC ( $J_{\text{CH}} = 140$  Hz), gHMBC ( $J_{\text{CH}} = 8.3$  Hz), and ROESY. HSQMBC was measured with 128 increments, 192 scans per increment, block size of 16K, and 1.0 s relaxation delay. HSQC-TOCSY was recorded with 256 increments, 72 scans per increment, block size of 32K, and 1.6 s relaxation delay. Low-resolution mass spectra were acquired using a TOF BioApplied spectrometer. High-resolution mass measurement was acquired on a Bruker Daltonics Apex III 4.7e Fourier transform mass spectrometer, fitted with an Apollo API source. A Betasil C18 column (5 mm, 150 × 21.2 mm) and Hypersil BDS C18 column (5 mm, 250 × 10 mm) were used for semipreparative HPLC. All solvents used for extraction and chromatography were Omnisolv HPLC grade, and the H<sub>2</sub>O used was Millipore Milli-Q PF filtered.

**Animal Material.** A specimen of *Neamphius huxleyi* was collected at the depth of 22 m, Milln Reef, off Cape Grafton, Queensland, Australia, in 2002. It was identified as *Neamphius huxleyi* (phylum Porifera, class Demospongiae, order Hadromerida, family Alectonidae). A voucher specimen (QMG319323) has been deposited at the Queensland Museum, South Brisbane, Queensland, Australia.

**Extraction and Isolation.** LC/MS analysis of the single active fraction of *N. huxleyi* extract indicated this fraction contained ion peaks at (+)  $m/z$  788.0, 788.5, and 795.0 in (+)-LRESIMS. A freeze-dried sample of *N. huxleyi* (5 g) was then extracted exhaustively with hexane (250 mL), CH<sub>2</sub>Cl<sub>2</sub> (250 mL), and MeOH (2 × 250 mL), respectively. The CH<sub>2</sub>Cl<sub>2</sub> and MeOH extracts were combined, and solvents were evaporated to yield a yellow residue (0.5 g). This extract was preadsorbed onto C18 (1 g) and packed dry into a small cartridge, which was connected to a C18 preparative HPLC column (5 mm, 21.2

× 150 mm). A linear gradient from 100% H<sub>2</sub>O (0.1% TFA) to 100% MeOH (0.1% TFA) was performed over 60 min at a flow rate of 9 mL/min, and 60 fractions (1.0 min each) were collected. Mass-guided identification demonstrated fractions 26 to 29 containing the ion peaks of interest at (+) *m/z* 795 and 788 by (+)-LRESIMS. <sup>1</sup>H NMR spectra of these fractions revealed impurities. Fractions 26 to 28 were then combined and chromatographed on a Betasil C18 column (5 mm, 150 × 21.2 mm) from 45% MeOH (0.1% FA)/55% H<sub>2</sub>O (0.1% FA) to 100% MeOH (0.1% FA) in 60 min to obtain 2 (12 mg, 0.24% dry wt) in fractions 46–48 and 3 (4 mg, 0.08% dry wt) in fractions 50–51. Fraction 29 was also purified on a Betasil C18 column (5 mm, 4.6 × 150 mm) from 50% MeOH (0.1% FA)/50% H<sub>2</sub>O (0.1% FA) to 100% MeOH (0.1% FA) in 30 min, yielding 4 (1.2 mg, 0.024% dry wt).

**Neamphamide B (2):** colorless, amorphous powder;  $[\alpha]_D^{24}$  –6 (c 0.08, MeOH); UV (MeOH)  $\lambda_{max}$  (log  $\epsilon$ ) 233 (3.8), 275 (3.1) nm; IR (film)  $\nu_{max}$  3315, 1740, 1659, 1510 cm<sup>-1</sup>; <sup>1</sup>H (600 MHz) and <sup>13</sup>C (150 MHz) NMR data are summarized in Table S1 (Supporting Information); (+) HRESIMS *m/z* 1574.8935 [M + H]<sup>+</sup> (calcd for [C<sub>71</sub>H<sub>120</sub>N<sub>19</sub>O<sub>21</sub>]<sup>+</sup>, 1574.8901,  $\Delta$  2.2 ppm).

**Neamphamide C (3):** colorless, amorphous powder;  $[\alpha]_D^{24}$  –8 (c 0.08, MeOH); UV (MeOH)  $\lambda_{max}$  (log  $\epsilon$ ) 233 (3.8), 275 (3.1) nm; IR (film)  $\nu_{max}$  3315, 1740, 1660, 1512 cm<sup>-1</sup>; <sup>1</sup>H (600 MHz) and <sup>13</sup>C (150 MHz) NMR data are summarized in Table S2 (Supporting Information); (+) HRESIMS *m/z* 1575.8726 [M + H]<sup>+</sup> (calcd for [C<sub>71</sub>H<sub>119</sub>N<sub>18</sub>O<sub>22</sub>]<sup>+</sup>, 1575.8741,  $\Delta$  –0.9 ppm).

**Neamphamide D (4):** colorless, amorphous powder;  $[\alpha]_D^{24}$  –19 (c 0.08, MeOH); UV (MeOH)  $\lambda_{max}$  (log  $\epsilon$ ) 233 (3.7), 275 (3.0) nm; IR (film)  $\nu_{max}$  3318, 1739, 1659, 1518 cm<sup>-1</sup>; <sup>1</sup>H (600 MHz) and <sup>13</sup>C (150 MHz) NMR data are summarized in Table S3 (Supporting Information); (+) HRESIMS *m/z* 1588.9052 [M + H]<sup>+</sup> (calcd for [C<sub>72</sub>H<sub>122</sub>N<sub>19</sub>O<sub>21</sub>]<sup>+</sup>, 1588.9057,  $\Delta$  –0.3 ppm).

**ESI-FTICR-MS<sup>n</sup> Analysis.** Mass spectrometric data were obtained in the positive ion mode on a Bruker Apex III 4.7 T, which was equipped with an ESI Apollo source. Samples were directly infused by a Cole-Parmer syringe pump with a flow rate of 2  $\mu$ L/min. The end plate or counter electrode voltage was biased at 3900 V and the capillary voltage at 4400 V relative to the ESI needle. N<sub>2</sub> gas was used as nebulizing gas with a pressure of 50 psi and as counter-current drying N<sub>2</sub> gas with a flow of 50 L/min. The drying gas temperature was maintained at 125 °C. The capillary exit voltage was tuned at 120 V. ESI mass spectra were recorded in the mass range *m/z* 50–3000 Da. SORI-CID was used for fragmentation in FTMS<sup>n</sup> experiments. Data acquisition and processing were performed using Xmass software.

Parameters for MS<sup>2</sup> were correlated sweep pulse length, 1000  $\mu$ s; correlated sweep attenuation, 21.4 dB; ejection safety belt, 0 Hz; user pulse length, 40 000  $\mu$ s; ion activation pulse length, 250 000  $\mu$ s; ion activation attenuation, 42.0 dB; frequency offset from activation mass, 500 Hz; user delay length, 10 s.

Parameters for MS<sup>3</sup> were correlated sweep pulse length, 600  $\mu$ s; correlated sweep attenuation, 42.5 dB; ejection safety belt, 0 Hz; user pulse length, 40 000  $\mu$ s; ion activation pulse length, 250 000  $\mu$ s; ion activation attenuation, 42.0 dB; frequency offset from activation mass, 500 Hz; user delay length, 10 s.

**Peptide Hydrolysis.** Peptide samples (200  $\mu$ g) were dissolved in degassed 6 N HCl (500  $\mu$ L) and heated at 120 °C for 16 h. The solvent was removed under dry nitrogen, and the resulting material was subjected to further derivatization for stereochemical assignment.

**LC/MS Analysis of Marfey's Derivatives.** A portion of the hydrolysate mixture (100  $\mu$ g) or the amino acid standard was added to a solution of L-FDAA 1% (w/w) in acetone containing 100  $\mu$ L of a 1 N NaHCO<sub>3</sub> solution. The vial was heated at 50 °C for 3 h, and the contents were neutralized with 0.2 N HCl (50  $\mu$ L) after cooling to room temperature. An aliquot of the L-FDAA derivative was dried under dry nitrogen, diluted in DMSO, and loaded on a Phenomenex Luna column (C18, 3 mm, 2.0 mm × 150 mm) using a linear gradient from 100% H<sub>2</sub>O (0.1% formic acid) to 100% CH<sub>3</sub>CN (0.1% formic acid) in 50 min and isocratic at 100% CH<sub>3</sub>CN (0.1% formic acid) for the next 10 min. FDAA derivatives were detected by UV absorption at 340 nm, and their assignments were secured by ion mass extraction.

Retention times of authentic FDAA-amino acids in minutes are given in parentheses: L-Arg (16.18), D-Arg (16.32), L-Asn (20.71), D-Asn (21.08), L-Hpr (27.03), D-Hpr (26.35), L-Leu (28.95), D-Leu (30.09), L-NMeGln (25.16), D-NMeGln (25.89), L-NMeGlu (25.71), D-NMeGlu (26.52), L-Thr (21.68), D-Thr (23.27), L-*a*Thr (21.24), and D-*a*Thr (22.54).

The hydrolysate of neamphamide B (2) contained D-Arg (16.35), L-Asn (20.74), L-Hpr (27.08), L-Leu (28.93), L-NMeGln (25.19), and D-*a*Thr (22.58).

The hydrolysate of neamphamide C (3) contained D-Arg (16.31), L-Asn (20.73), L-Hpr (27.03), L-Leu (28.94), L-NMeGlu (25.75), and D-*a*Thr (22.55).

The hydrolysate of neamphamide D (4) contained D-Arg (16.34), L-Asn (20.75), L-Hpr (27.06), L-Leu (28.95), L-NMeGln (25.20), and D-*a*Thr (22.59).

**Cytotoxicity Assay.** Noncancer cell lines human embryonic kidney (HEK 293) and human neonatal foreskin fibroblasts (NFF) along with human lung adenocarcinoma cells (A549) were grown in media: DMEM supplemented with 10% fetal bovine serum (FBS), 100 units/mL penicillin, and 100  $\mu$ g/mL streptomycin. Cervical adenocarcinoma cells (HeLa) and the prostate adenocarcinoma cells (LNCaP and PC3) were grown in media: RPMI supplemented with 10% FBS, 100 units/mL penicillin, and 100  $\mu$ g/mL streptomycin. Cells were grown under 5% CO<sub>2</sub> in a humidified environment at 37 °C. Compound toxicity was measured after 72 h incubation using an Alamar blue proliferation assay. Forty-five microliters of media containing 1000 cells was added to a 384-well microtiter plate (Falcon black clear 384 TC microtiter plates). Plates were incubated overnight at 37 °C, 5% CO<sub>2</sub>, and 80% humidity to allow cells to adhere. Stock concentrations of pure compounds were prepared at 10 mM in 100% DMSO. Compounds were then diluted 1 in 10 in media. Five microliters of diluted compound were added to the cells to give a total volume of 50  $\mu$ L. Final compound concentration range tested was 100  $\mu$ M to 3 nM (final DMSO concentration of 1%). Each concentration in media was tested in triplicate. Cells and compounds were then incubated for 72 h at 37 °C, 5% CO<sub>2</sub>, and 80% humidity. Cell proliferation was measured with the addition of 10  $\mu$ L of a 60% Alamar blue solution in media to each well of the microtiter plate to give a final concentration of 10%. The plates were incubated at 37 °C, 5% CO<sub>2</sub>, and 80% humidity for 24 h. The fluorescence of each well was read at excitation 535 nm and emission 590 nm on a Victor II Wallac plate reader (PerkinElmer, USA). Ten-point concentration response curves were then analyzed using nonlinear regression and IC<sub>50</sub> values determined by using GraphPad Prism 5. Vincristine sulfate was used during each screening run as a positive control compound.

**xCelligence Assay.** The xCelligence RTCA system (Roche) has been described previously. For our experiments, 100  $\mu$ L of media was added to each well of the 96-well E-plate to measure background levels of impedance. After measuring the background, 100  $\mu$ L of cell suspension was added to reach a cell density of 4000 cells/well. Cells were allowed to seed at room temperature for 30 min and then placed in the reader at 37 °C and 5% CO<sub>2</sub> for real-time recording of the cell index. The following day, half of the media was removed and replaced with the corresponding volume (100  $\mu$ L) of media with 2× concentrated compound in order to reach the desired concentration in the well. Negative controls were treated with the vehicle (DMSO at 1% final concentration). Each condition was tested in triplicates and in two independent experiments. The cells were monitored every minute for the first 2 h after treatment and every hour until 72 h after treatment.

## ■ ASSOCIATED CONTENT

### 📄 Supporting Information

NMR and ESI-FTICR-MS<sup>n</sup> spectra for 2–4 and a photograph of the sponge *Neamphius huxleyi* are available free of charge via the Internet at <http://pubs.acs.org>.

## AUTHOR INFORMATION

### Corresponding Author

\*Tel: +61-7-3735-6009. Fax: +61-7-3735-6001. E-mail: r. quinn@griffith.edu.au.

### Notes

The authors declare no competing financial interest.

## ACKNOWLEDGMENTS

One of the authors (T.D.T.) acknowledges Education Australia Ltd for the provision of the “EAL Postgraduate Research Student Mobility Scholarships”. We also thank Assoc. Prof. A. Hoffmann and Ms. A. Osman for the support of authentic amino acid standards and Ms. B. Aldred for the provision of cancer cell lines.

## REFERENCES

- (1) Zampella, A.; D'Auria, M. V.; Paloma, L. G.; Casapullo, A.; Minale, L.; Debitus, C.; Henin, Y. *J. Am. Chem. Soc.* **1996**, *118*, 6202–6209.
- (2) D'Auria, M. V.; Zampella, A.; Paloma, L. G.; Minale, L.; Debitus, C.; Roussakis, C.; Bert, V. L. *Tetrahedron* **1996**, *52*, 9589–9596.
- (3) Zampella, A.; Randazzo, A.; Borbone, N.; Luciani, S.; Trevisi, L.; Debitus, C.; D'Auria, M. V. *Tetrahedron Lett.* **2002**, *43*, 6163–6166.
- (4) Sepe, V.; D'Orsi, R.; Borbone, N.; D'Auria, M. V.; Bifulco, G.; Monti, M. C.; Catania, A.; Zampella, A. *Tetrahedron* **2006**, *62*, 833–840.
- (5) D'Auria, M. V.; Sepe, V.; D'Orsi, R.; Bellotta, F.; Debitus, C.; Zampella, A. *Tetrahedron* **2007**, *63*, 131–140.
- (6) Zampella, A.; Sepe, V.; Luciano, P.; Bellotta, F.; Monti, M. C.; D'Auria, M. V.; Jepsen, T.; Petek, S.; Adeline, M. T.; Laprévôte, O.; Aubertin, A. M.; Debitus, C.; Poupat, C.; Ahond, A. *J. Org. Chem.* **2008**, *73*, 5319–5327.
- (7) Zampella, A.; Sepe, V.; Bellotta, F.; Luciano, P.; D'Auria, M. V.; Cresteil, T.; Debitus, C.; Petek, S.; Poupat, C.; Ahond, A. *Org. Biomol. Chem.* **2009**, *7*, 4037–4044.
- (8) Plaza, A.; Gustchina, E.; Baker, H. L.; Kelly, M.; Bewley, C. A. *J. Nat. Prod.* **2007**, *70*, 1753–1760.
- (9) Ford, P. W.; Gustafson, K. R.; McKee, T. C.; Shigematsu, N.; Maurizi, L. K.; Pannell, L. K.; Williams, D. E.; Silva, E. D. D.; Lassota, P.; Allen, T. M.; Soest, R. V.; Andersen, R. J.; Boyd, M. R. *J. Am. Chem. Soc.* **1999**, *121*, 5899–5909.
- (10) Ratnayake, A. S.; Bugni, T. S.; Feng, X.; Harper, M. K.; Skalicky, J. J.; Mohammed, K. A.; Andjelic, C. D.; Barrows, L. R.; Ireland, C. M. *J. Nat. Prod.* **2006**, *69*, 1582–1586.
- (11) Oku, N.; Gustafson, K. R.; Cartner, L. K.; Wilson, J. A.; Shigematsu, N.; Hess, S.; Pannell, L. K.; Boyd, M. R.; McMahan, J. B. *J. Nat. Prod.* **2004**, *67*, 1407–1411.
- (12) Hooper, J. N. A.; Soest, R. W. M. V. *Systema Polifera: A Guide to the Classification of Sponges*; Kluwer Academic & Plenum: New York, 2002.
- (13) Silva, E. D. D.; Racok, J. S.; Andersen, R. J.; Allen, T. M.; Brinen, L. S.; Clardy, J. *Tetrahedron Lett.* **1991**, *32*, 2707–2710.
- (14) Marfey, P. *Carlsberg Res. Commun.* **1984**, *49*, 591–596.
- (15) Matsumori, N.; Kaneno, D.; Murata, M.; Nakamura, H.; Tachibana, K. *J. Org. Chem.* **1999**, *64*, 866–876.
- (16) Riccio, R.; Bifulco, G.; Cimino, P.; Bassarello, C.; Paloma, L. G. *Pure Appl. Chem.* **2003**, *75*, 295–308.
- (17) Bifulco, G.; Dambruoso, P.; Paloma, L. G.; Riccio, R. *Chem. Rev.* **2007**, *107*, 3744–3779.
- (18) Oku, N.; Krishnamoorthy, R.; Benson, A. G.; Ferguson, R. L.; Lipton, M. A.; Phillips, L. R.; Gustafson, K. R.; McMahan, J. B. *J. Org. Chem.* **2005**, *70*, 6842–6847.
- (19) Zampella, A.; D'Orsi, R.; Sepe, V.; Casapullo, A.; Monti, M. C.; D'Auria, M. V. *Org. Lett.* **2005**, *7*, 3585–3588.
- (20) *Dictionary of Natural Products on CD-Rom*; Chapman and Hall/CRC Press: London, UK, 2012.
- (21) Abassi, Y. A.; Xi, B.; Zhang, W.; Ye, P.; Kirstein, S. L.; Gaylord, M. R.; Feinstein, S. C.; Wang, X.; Xu, X. *Chem. Biol.* **2009**, *16*, 712–723.
- (22) Ke, N.; Xi, B.; Ye, P.; Xu, W.; Zheng, M.; Mao, L.; Wu, M. J.; Zhu, J.; Wu, J.; Zhang, W.; Zhang, J.; Irelan, J.; Wang, X.; Xu, X.; Abassi, Y. A. *Anal. Chem.* **2010**, *82*, 6495–6503.